

## Natural scene statistics at the centre of gaze

Pamela Reinagel<sup>†</sup>§ and Anthony M Zador<sup>‡</sup>||

<sup>†</sup> Sloan Center for Theoretical Neuroscience, California Institute of Technology, Pasadena, CA 91125, USA

<sup>‡</sup> Salk Institute MNL/S, La Jolla, CA 92037, USA

E-mail: pam@v1.med.harvard.edu

Received 20 January 1999

**Abstract.** Early stages of visual processing may exploit the characteristic structure of natural visual stimuli. This structure may differ from the intrinsic structure of natural scenes, because sampling of the environment is an active process. For example, humans move their eyes several times a second when looking at a scene. The portions of a scene that fall on the fovea are sampled at high spatial resolution, and receive a disproportionate fraction of cortical processing. We recorded the eye positions of human subjects while they viewed images of natural scenes. We report that active selection affected the statistics of the stimuli encountered by the fovea, and also by the parafovea up to eccentricities of 4°. We found two related effects. First, subjects looked at image regions that had high spatial contrast. Second, in these regions, the intensities of nearby image points (pixels) were less correlated with each other than in images selected at random. These effects could serve to increase the information available to the visual system for further processing. We show that both of these effects can be simply obtained by constructing an artificial ensemble comprised of the highest-contrast regions of images.

### 1. Introduction

The visual world in which humans have evolved is highly structured, not random like the static observed on an untuned television monitor. Simple statistical analyses reveal robust invariances across natural images [1–4], such as a strong correlation in the intensity of nearby points. Such invariances can be used to encode visual stimuli more efficiently. For example, the encoding of any stimulus ensemble is most efficient if the dynamic range of the neural response is allocated preferentially to those aspects of the stimuli that vary most. Thus it has been proposed that sensory systems have specifically evolved to encode their natural stimuli efficiently, by taking advantage of stimulus invariances [5, 6]. There is recent evidence for this hypothesis in the computations performed by the first stages of visual systems [7–19].

Visual systems may be adapted not only to the structure found in natural images, but also to the structure imposed by the organism's own actions. In insects, for example, visual motion detectors are matched to the speed of flight and thus to the temporal frequencies typically experienced [20, 21]. Similarly, human eye movements influence the statistics of the effective visual input. Humans move their eyes several times a second when looking at a scene. The portions of a scene that fall on the fovea are sampled at high spatial resolution, and receive a disproportionate fraction of cortical processing.

§ Author to whom any correspondence should be addressed. Current address: Department of Neurobiology, Harvard Medical School, 220 Longwood Avenue, Boston, MA 02115, USA; telephone: (617) 432-3622; fax: (617) 734-7557.

|| Present address: Cold Spring Harbor Laboratory, 1 Bungtown Road, Cold Spring Harbor, NY 11724, USA.

To date, studies relating receptive field properties of early visual neurons to natural scene statistics have implicitly assumed that the visual world is sampled uniformly. However, it is clear that eye movements alter the statistics of the input reaching the fovea. For example, one well-known finding about eye movements is that humans tend to look at faces when these are present in an image [22]. From this one might suspect that a face-responsive neuron responds more often than would be predicted on the basis of the frequency of faces in natural scenes.

Early visual neurons respond to stimulus features much simpler than faces. In this study we ask whether voluntary eye movements change the statistics of simple, local spatial properties of images (see also [23–25]). If so, then to test the theory that early visual neurons are optimized for their natural visual input, eye movements must be included in the description of that input.

## 2. Methods

### 2.1. Protocol

An RK-416 infrared Pupil Tracking System (Iscan Incorporated, Cambridge, MA) was used to record eye position every 20 ms. A bite bar was used to minimize head movement. Subjects viewed the images on a 21-inch monitor at 79 cm; the whole image subtended  $28^\circ \times 21^\circ$  of visual angle (23 pixels/degree). Subjects were instructed to ‘study the images’. Images were presented in seven blocks of eleven images each. Within a block, a brief central fixation cue preceded each 10 s image presentation. Raw eye positions were corrected by linear interpolation using a  $5 \times 5$  calibration grid presented before each image block. The estimated tracking error was less than  $0.5^\circ$  of visual angle. The analysis shown is based on eye positions from 0.4–4 s after presentation of the image. The first 0.4 s were omitted to avoid any bias due to the central fixation cue preceding each image. We focused on the first 4 s because, anecdotally, effects diminished gradually with viewing time.

### 2.2. Image ensemble

Seventy-seven images were presented to five naive subjects. All images were  $640 \times 480$  pixels, with 256 grey levels. The image ensemble included 69 natural images, of which 38 depicted nature scenes, 17 depicted man-made objects such as building interiors and exteriors, and 14 included animals or humans. Images with substantial blank areas were explicitly excluded from our ensemble. All images were in sharp focus at all depths of field. These images were amateur and professional black-and-white photographs from a variety of sources, scanned on a Scanjet 4c Digitizer (Hewlett-Packard). The results in this paper were based on the 69 natural images; analysis of the remaining eight synthetic images is not included.

### 2.3. Definitions

We use the term ‘contrast’ to refer to the local standard deviation within a patch, normalized by the global mean intensity of the image. We use  $\Pi_1, \dots, \Pi_N$  to denote the indices  $(i, j)$  of the  $23^2$  pixels in a  $1^\circ$  ( $23 \times 23$  pixel) square image patch centred on the  $N$  eye positions. The unitless contrast  $C$  was then defined for each image as

$$C = \bar{I}^{-1} N^{-1} \sum_k \left[ \sum_{(i,j) \in \Pi_k} (I_{ij} - \bar{I}_k)^2 \right]^{1/2}$$

where  $I_{ij}$  is the intensity of the pixel at position  $(i, j)$ ,  $\bar{I}_k$  is the mean intensity of the  $k$ th patch, and  $\bar{I}$  is the mean intensity of the entire image. For the reference ensemble  $\mathcal{R}$ , random eye positions from the reference ensemble drawn were substituted for subjects’ eye positions.

Local measures of contrast are problematic because they depend on an arbitrary choice of spatial scale (but see [26–28]). Our ‘contrast’ measure simply reflects the variance of the local pixel intensities, on the spatial scale of the size of the fovea. We normalized to the mean intensity of the entire image, but only to provide a unitless measure. We emphasize that we have *not* normalized to the local mean, even though the local variance is expected to be correlated with the local mean intensity due to the effects of illumination. Therefore our ‘contrast’ reflects both variance due to illumination of the scene and variance due to intrinsic properties of the objects in the scene. In other calculations, not shown, we found that variance was more strongly and more consistently related to eye positions than either the local mean intensity or a locally normalized contrast.

Spatial correlations are among the best-studied statistics of natural images. These correlations are often expressed in terms of Fourier spectral analysis [1–4]. The power spectrum of an image is a direct restatement of the spatial correlation function, but only when the image samples are translation invariant. This condition was met in past studies that assumed uniform sampling of natural scenes. However, in the subject-selected ensemble  $\mathcal{S}$ , translation invariance was explicitly violated: the centre of each patch is by definition a privileged point, and the properties in the centre of patches may therefore differ systematically from the properties at the edges. Because translation invariance cannot be assumed for the ensemble  $\mathcal{S}$ , we describe spatial correlations in the spatial domain for all ensembles.

We define the unnormalized two-point *correlation function*  $r(i, j, i', j')$  of two points  $(i, j)$  and  $(i', j')$  over an ensemble of  $N$  patches as

$$r(i, j, i', j') = N^{-1} \left[ \sum_k (I_{ijk} - \tilde{I}_{ij})(I_{i'j'k} - \tilde{I}_{ij}) \right]^{1/2}$$

where  $I_{ijk}$  is the intensity of the point  $(i, j)$  in the  $k$ th patch and

$$\tilde{I}_{ij} = N^{-1} \sum_k I_{ijk}$$

is the mean intensity at this position averaged over patches. The normalized correlation function was defined to be unity for the autocorrelation of the central pixel,

$$\rho(i, j, i', j') = r(i, j, i', j')/r(0, 0, 0, 0).$$

For notational convenience, the indices of  $\rho$  have been omitted in the body of the text where there is no risk of ambiguity. Unlike contrast, the correlation function is not defined for individual patches, but rather is computed from an ensemble of patches from one image.

We note that the normalization  $r(0, 0, 0, 0)$  depends only on the variability (over the ensemble, and not over space) of the central pixel. As a result, this normalization does not depend on the size of the patch used. If instead the spatial contrast  $C$  shown in figure 2(A)—see later—were used, the correlation function would depend on the size of the patch used to calculate it.

#### 2.4. Entropy

We estimated the *entropy*  $H$  of each image ensemble by assuming that pixel intensities were drawn from a Gaussian distribution, using the expression (see reference [29])

$$H = 2^{-1} \left[ \sum_{i=1}^n \log(1 + \gamma_i/\eta) + n \log(2\pi e) \right]$$

where  $\gamma_i$  are the eigenvalues of the  $n \times n$  covariance matrix derived from a vertical and horizontal slices through the middle of each patch, and  $\eta$  is a ‘noise’ level related to the quantization of

pixel intensity. The covariance matrices for the subject-selected ensemble were obtained by averaging together the results from all five subjects.

Because the distribution of eigenvalues in natural images is not Gaussian, this method overestimates the entropy. However, in the present study we are interested in the *difference* between the entropy of the subject-selected and randomly sampled ensembles. Thus to the extent that the coefficient distributions deviate from Gaussian in the same way, the difference is not very sensitive to the details of the distribution. As an independent check, the entropies were also computed by explicitly computing the entropy of wavelet coefficient distributions (analogous to the eigenvalue distribution), and similar results were obtained (*not shown*).

### 3. Results

We recorded eye positions from subjects as they viewed static black-and-white images presented on a computer monitor (see section 2). One such image, with the superimposed eye positions from one subject, is shown in figure 1. Every 20 ms we extracted a fovea-sized square image *patch* ( $1^\circ \times 1^\circ$ , i.e.  $23 \times 23$  pixels) around the subject's centre of gaze. The ensemble  $\mathcal{S}(i)$  of such patches approximates the input to the subject's fovea for the  $i$ th image. We compared  $\mathcal{S}(i)$  to a reference ensemble  $\mathcal{R}(i)$ , which was constructed of image patches selected at random (i.e. drawn from a spatially uniform distribution). The ensemble  $\mathcal{R}(i)$  represents the null hypothesis of uniform sampling.

#### 3.1. Contrast

We first compared the contrast (see section 2) of patches in the centre of gaze to that expected from random sampling. Figure 2(A) shows that in the majority of images (52/69, 75%,  $p < 0.001$ , two-sided sign test), the contrast in the subject-selected ensemble  $\mathcal{S}(i)$  was higher than in the reference ensemble  $\mathcal{R}(i)$  drawn from the same image. On average, the contrast of  $\mathcal{S}(i)$  was 1.20-fold higher than that of  $\mathcal{R}(i)$ . Thus, subjects looked preferentially at parts of an image with higher spatial contrast.

With the contrast measure we used, local luminance is expected to covary with local contrast, and indeed there was an increase in local mean luminance in the subject-selected ensemble  $\mathcal{S}(i)$ . If local contrast was instead normalized to the local mean, removing effects due to illumination,  $\mathcal{S}(i)$  still showed a net increase in this locally normalized contrast, but the effect was far more variable across images and subjects, and was not by itself statistically significant. The simple measure that we used appeared to be more consistently related to eye position than either mean or locally normalized contrast.

The subject-selected ensemble  $\mathcal{S}$  showed a bias for the centre of the images. We found that contrast was also higher, on average, near the centre of the images. To see if an intrinsic bias for looking in the centre could account for our result, we created a control ensemble for each image,  $\mathcal{U}(i)$ , in which eye positions were shuffled, i.e., real eye positions generated while viewing another image were used to select patches from the image  $i$ . The contrast in  $\mathcal{S}(i)$  was on average 1.17-fold higher than in the image-shuffled control  $\mathcal{U}(i)$  (increase observed in 50/69, or 72%, of images,  $p < 0.001$ , two-sided sign test). Thus, the effect we observed was due primarily to specific eye positions, rather than a bias for looking in the middle.

#### 3.2. Correlation

Contrast is a measure of the variability of the intensity within an image patch. Contrast is, however, insensitive to the spatial organization of intensities within the patch. For example,

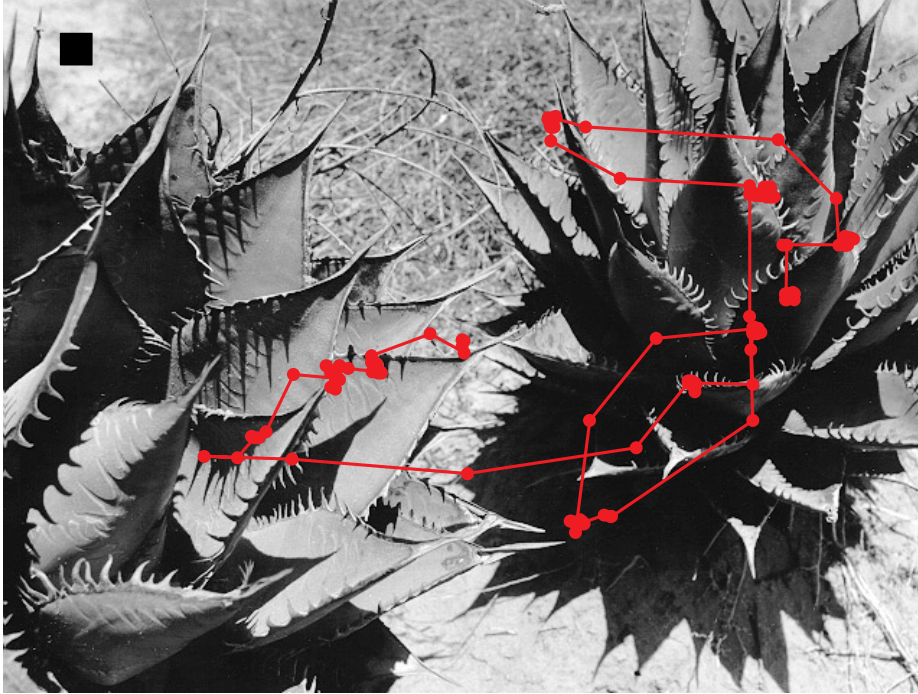


**Figure 1.** A representative image from our ensemble with eye positions of one subject superimposed. The red circles indicate the position of the centre of gaze recorded at 20 ms intervals. The calibration square in the upper left corner is  $1^\circ \times 1^\circ$  of visual angle.

consider a patch in which there are an equal number of black and white pixels, arranged in clumps. In such a patch, if a particular pixel is black, its neighbour is probably black as well. If the pixels in this patch were scrambled, the contrast would be unchanged, but the neighbour of a black pixel would now be just as likely to be white as black. Thus contrast and spatial correlation can be varied separately.

We used the correlation function  $\rho$  to quantify the correlation in intensity between pairs of pixels in the image (see section 2). For perfectly correlated points  $\rho = 1$ , while for uncorrelated points  $\rho = 0$ . In general,  $\rho$  is a function of the distance  $\Delta$  between image points (pixels). For a clumpy image, nearby points show strong correlations, so  $\rho$  decreases only gradually with distance. As illustrated in figure 2(B), in natural images the correlation between two points typically decreases as the distance  $\Delta$  between them increases, with perfect correlation by definition when  $\Delta = 0$ . However, in the subject-selected image ensemble ( $\mathcal{S}$ ), nearby points are less correlated ( $\rho$  decreases more rapidly) than in either the randomly sampled ( $\mathcal{R}$ ) or image-shuffled ( $\mathcal{U}$ ) control ensembles. (A parsimonious explanation of the difference between  $\mathcal{U}$  and  $\mathcal{R}$  is that when photographers point their cameras, they are influenced by the same cues as subjects when they direct their gaze.) Thus active selection changes not only the contrast, but also the spatial correlation  $\rho$ , at the fovea.

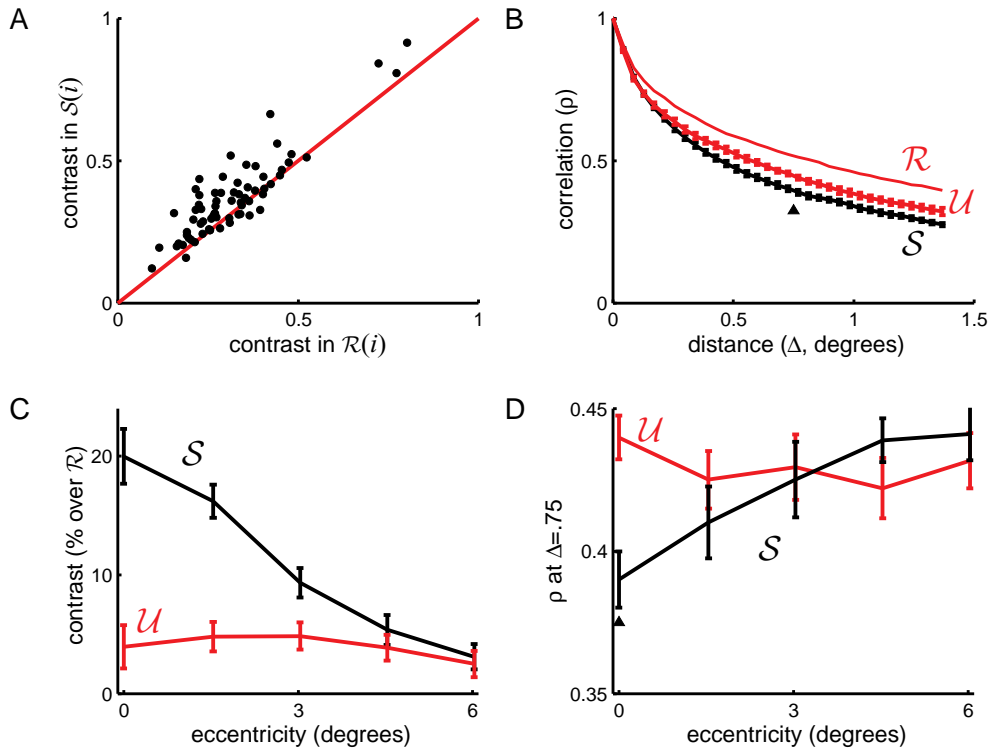


**Figure 2.** The spatial statistics of patches in the subject-selected ensemble differ from those of patches selected at random. (A) For each image  $i$ , a single point is plotted showing the average contrast of a fovea-sized ( $1^\circ$ ) patch in  $\mathcal{R}(i)$  on the abscissa, and of a patch in  $\mathcal{S}(i)$  (averaged over all subjects) on the ordinate. Points above the diagonal indicate that contrast of patches in the subject-selected ensemble  $\mathcal{S}(i)$  is higher than that of patches in the reference ensemble  $\mathcal{R}(i)$ . The mean contrast for  $\mathcal{R}$  was 0.32 (range: 0.09–0.80), for  $\mathcal{S}$  was 0.37 (range: 0.12–0.91), and for  $\mathcal{U}$  (not shown) was 0.33 (range: 0.09–0.88). (B) Nearby points in the subject-selected ensemble are less correlated than in the reference ensembles. The correlation  $\rho$  between the point at the centre of each patch and a point  $\Delta$  degrees away is plotted as a function of  $\Delta$ . The three curves represent the correlation functions for the uniformly sampled ensemble  $\mathcal{R}$  (upper), the image-shuffled ensemble  $\mathcal{U}$  (middle), and the subject-selected ensemble  $\mathcal{S}$  (lower), averaged over all images and subjects. Within each ensemble, a normalized correlation function was computed separately for each image, based on points displaced from the centre in each of four directions ( $0^\circ$ ,  $90^\circ$ ,  $180^\circ$  and  $270^\circ$ ). These normalized correlation functions were then averaged over images. Error bars indicate the standard error between subjects. Note that points along the abscissa are separated by 1 pixel =  $1/23^\circ$ . (C) The effect on contrast decays over about  $4^\circ$  eccentricity. The contrast effect (% increase over the  $\mathcal{R}$  baseline) of patches centred on points  $\Delta$  degrees eccentric to the subject-selected eye positions is plotted as a function of  $\Delta$ . The curve decays to the image-shuffled control ensemble  $\mathcal{U}$  (red line). Error bars indicate standard errors over subjects. (D) The correlation function decays within an eccentricity of about  $2^\circ$ . The correlation  $\rho$  between a point P located  $\epsilon$  degrees eccentric to the centre of each patch, and point P' located  $\Delta = 0.75^\circ$  more eccentric (i.e. along the vector from the origin of the patch to the point P), is plotted as function of the eccentricity  $\epsilon$  from the centre of the fovea. The scale is expanded to show detail. The 0 eccentricity point (arrow) corresponds to the same data as are marked by an arrow in (B). The red line indicates the result as a function of eccentricity for the image-shuffled control ensemble  $\mathcal{U}$ . The correlation of  $\mathcal{R}$  is off the scale (see (B)). The correlation functions were computed as in (B). The curve represents the average over five subjects and four directions ( $0^\circ$ ,  $90^\circ$ ,  $180^\circ$  and  $270^\circ$ ) away from the centre of each patch.

### 3.3. Eccentricity

To determine how far from the fovea these effects extended, we measured the statistics of image patches falling in parafoveal fields. For each eccentricity, we created an ensemble of image patches centred on points a fixed distance from the centre of gaze. The contrast of the subject-selected ensemble  $\mathcal{S}$  remained higher than that of  $\mathcal{U}$  up to an eccentricity of about four degrees from the fovea (figure 2(C)). The effect on the two-point correlation  $\rho$  diminished gradually over about two degrees from the fovea, as shown for one distance ( $\Delta = 0.75$ ) in figure 2(D). Thus eye movements changed the statistics of the visual input within the central  $8^\circ$  of the visual field.

Our measurement of individual eye positions is subject to an error of about  $\pm 0.5^\circ$ . This error probably caused us to underestimate the magnitude of the effects at the fovea, because results from the foveal image patches were averaged with patches as much as  $0.5^\circ$  eccentric. The approximate magnitude of the underestimate can be inferred from figure 2, in which contrast (figure 2(C)) and correlation (figure 2(D)) are plotted as functions of eccentricity; the underestimate is probably less than 20%.

### 3.4. Artificial ensembles

We have identified two differences between the image regions where people looked ( $\mathcal{S}$ ) and image regions chosen at random ( $\mathcal{R}$ ). First, the average contrast of  $\mathcal{S}$  was greater than  $\mathcal{R}$ ; and second, nearby points in  $\mathcal{S}$  were less correlated than in  $\mathcal{R}$ . As noted in the example above, contrast does not, in general, specify the spatial organization of pixels within a patch, so one result need not imply the other. It could be, however, that because of some additional statistical structure intrinsic to natural images, pixels in high-contrast patches tend to be less correlated than in low contrast patches. If this were true, then an ensemble specifically selected for high contrast would also have a steeper correlation function  $\rho(\Delta)$ .

In order to test this possibility, we constructed an artificial ensemble  $\mathcal{A}$  comprised of the patches with the highest contrast. For each image, a contrast map was constructed by replacing the intensity of each pixel by the contrast  $C$  of the fovea-sized ( $1^\circ$ ) patch centred on that pixel. Figure 3(A) shows the contrast map of the same image as shown in figure 1, where intensity now represents contrast. The highest-contrast patches—the peaks from figure 3(A)—were then assembled to form the artificial maximum-contrast ensemble  $\mathcal{A}$  (figure 3(B)). By construction, the contrast of  $\mathcal{A}(i)$  was higher than that of  $\mathcal{R}(i)$  for every image (figure 3(C)), with an average 1.9-fold increase. Figure 3(D) shows that the two-point correlation coefficient  $\rho$  for this artificial ensemble is steeper than that of  $\mathcal{R}$ , demonstrating that high contrast is indeed associated with a steep correlation function in our images. Thus, selecting the highest-contrast image patches is sufficient to produce the change in the two-point function that we observed.

## 4. Discussion

We have examined how active visual sampling of natural scenes changes the simple statistics of the stimulus ensemble centred on the fovea. We have described two related effects: the image patches selected for viewing had (1) higher local spatial contrast and (2) a steeper two-point correlation function than patches selected at random. We further showed that an artificial ensemble constructed of the patches with the highest spatial contrast also had a steeper two-point correlation function.

In principle, contrast and spatial correlation can vary independently: as in the example discussed above, if black and white pixels are arranged in clumps, then the spatial correlation

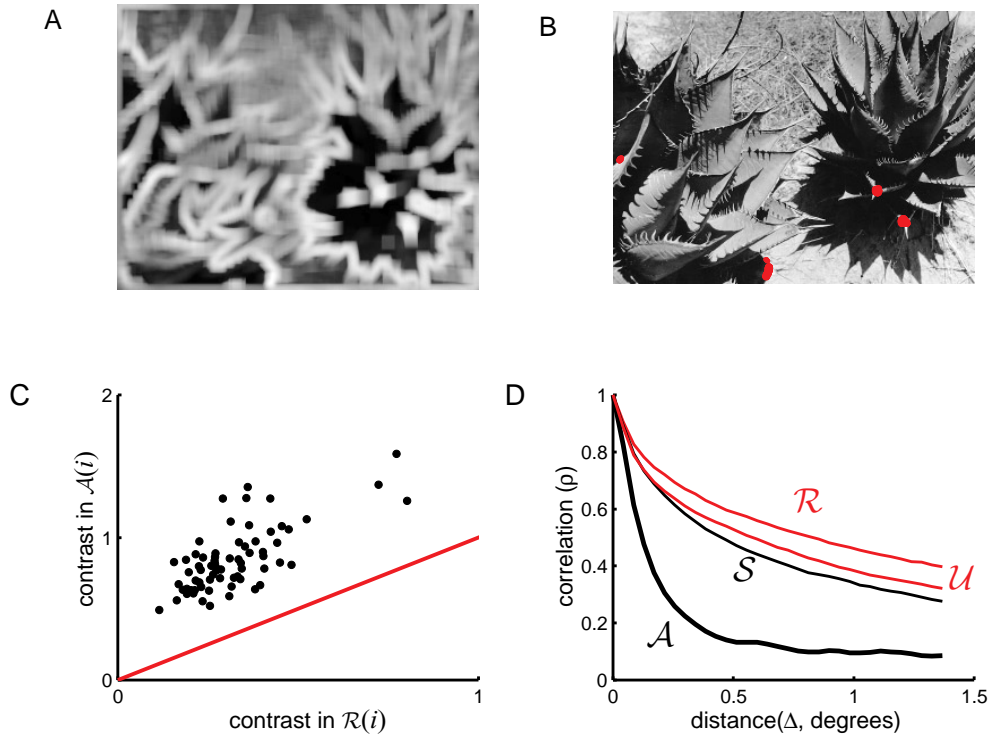


**Figure 3.** High-contrast artificial ensembles show reduced spatial correlations. (A) A contrast map of the image in figure 1. The contrast of a fovea-sized ( $1^\circ$ ) block centred on each pixel in figure 1 is represented by brightness. The mean contrast for  $\mathcal{A}$  was 0.84 (range: 0.84–1.59). (B) The 180 points of highest contrast are indicated by circles as in figure 1. These points represent the maximum-contrast ensemble of artificial ‘eye positions’ used in (C) and (D). (C) The contrast of randomly selected patches (abscissa) is compared with that of the maximum-contrast ensemble (ordinate) for each image. (D) Nearby points in the maximum-contrast ensemble are much less correlated for a given distance  $\Delta$  ( $\mathcal{A}$ ) than are points selected at random ( $\mathcal{R}$ ). Results from  $\mathcal{U}$  and  $\mathcal{S}$  are exactly as in figure 2(B), shown here for purposes of comparison.

will fall off more gradually than if they are distributed uniformly throughout the image, even though the total contrast may be identical.

However, our results imply an additional property of natural images: high local contrast is correlated with steeper two-point correlation functions. This statistical property of images has not been previously reported, and we were not able to derive it formally from those that have been reported. We can nevertheless advance an intuitive explanation: given that the world is composed of objects that are localized in space and relatively uniform in material composition, it would not be surprising if intensities in natural images are correlated mostly within objects, and if large differences in intensity occur mainly at the borders between objects. If so, contrast would be high, and the correlation  $\rho$  would be low, whenever a sample is centred on the border between different objects. We have not determined whether the effects that we observed in  $\mathcal{S}$  were caused by a preference of subjects for high contrast, for low correlation, or for something else correlated with these, such as edges. The underlying mechanism might be further elucidated using artificial images, in which contrast, correlation and other image properties could be manipulated independently.



Whatever the cause of subjects' selections, one can ask whether the consequences of these selections provide any advantage for the task of gathering information about a visual scene. One interpretation of the increase in the correlation coefficient  $\rho$  is that people use their fovea to examine details in regions of an image where the correlations between nearby pixels are weak, i.e. where there is rich structure on small spatial scales. Another, compatible interpretation is that this reflects an adaptation to maximize the information [29] available to early stages of visual processing. Higher-contrast patches have more variability in intensity, and a steeper correlation function means that intensities are less predictable from neighbouring intensities. Thus both the effects that we observe suggest an increase in the entropy of the effective visual input. Indeed, a comparison based on a simple estimate revealed a small (average increase of 0.1 bit/pixel out of 4.5 bit/pixel) but consistent ( $51/69 = 75\%$  of images) increase in the entropy of the subject-selected ensemble  $S$  compared to  $\mathcal{R}$  (see section 2).

We conclude that eye movements change visual input, not only for complex features like faces, but also for simple local properties like contrast and spatial correlation. Thus eye movements might serve to increase the information content of the visual input at multiple levels. Our results complement those of previous studies showing that subjects preferentially direct their gaze at parts of natural images rated high according to a subjective measure of informativeness [30], or according to a related measure of cognitive surprise (e.g. an octopus in a farm scene) [31]. Similarly, in reading tasks, mean fixation time on infrequent (surprising) words is longer than on the more frequent controls [32]. We do not suppose that image contrast or correlation explains these data. Rather, we assume that there is a competition between top-down and bottom-up cues for control of visual attention [33]. It has been suggested that bottom-up cues dominate during the first few seconds of viewing a new scene [34]. Additional experiments are needed to determine how stimulus cues and cognitive tasks interact to determine viewing dynamics, and to explore the effects of eye movements on temporal aspects of the stimulus [23].

## References

- [1] Ruderman D L and Bialek W 1994 *Phys. Rev. Lett.* **73** 814–17
- [2] Field D J 1987 *J. Opt. Soc. Am. A* **4** 2370–93
- [3] Tolhurst D J, Tadmor Y and Chao T 1992 *Ophthalm. Physiol. Opt.* **12** 229–32
- [4] van der Schaaf A and van Hateren J H 1996 *Vision Res.* **28** 2759–70
- [5] Atteneave F 1954 *Psychol. Rev.* **61** 183–93
- [6] Barlow H B 1961 *Sensory Communication* ed W Rosenblith (Cambridge, MA: MIT Press) pp 217–34
- [7] Atick J 1992 *Network* **3** 213–51
- [8] Bialek W and Zee A 1990 *J. Stat. Phys.* **59** 103–15
- [9] Li Z-P 1996 *Neural Comput.* **8** 705–30
- [10] Dong D W and Atick J J 1995 *Network* **6** 345–58
- [11] Dong D W and Atick J J 1995 *Network* **6** 159–78
- [12] Srinivasan M, Laughlin S and Dubs A 1982 *Proc. R. Soc. B* **216** 427–59
- [13] Olshausen B and Field D 1996 *Nature* **381** 607–9
- [14] Field D J 1994 *Neural Comput.* **6** 559–601
- [15] Bell A and Sejnowski T 1997 *Vision Res.* **37** 3327–38
- [16] Hateren J and van der Schaaf A 1998 *Proc. R. Soc. B* **265** 359–66
- [17] Blais B S, Intrator N, Shouval H and Cooper L N 1998 *Neural Comput.* **10** 1797–813
- [18] Shouval H, Intrator N and Cooper L N 1997 *Vision Res.* **37** 3339–42
- [19] Law C C and Cooper L N 1994 *Proc. Natl Acad. Sci. USA* **91** 7797–801
- [20] O'Carroll D C, Bidwell N, Laughlin S B and Warrant E J 1996 *Nature* **382** 63–6
- [21] O'Carroll D C, Laughlin S, Bidwell N and Harris R 1997 *Vision Res.* **37** 3427–39
- [22] Yarbus A L 1967 *Eye Movements and Vision* (New York: Plenum)
- [23] Eckert M and Buchsbaum G 1993 *Phil. Trans. R. Soc. B* **339** 385–95
- [24] Mannan S, Ruddock K and Wooding D 1997 *Perception* **26** 1059–72

- [25] Mannan S, Ruddock K and Wooding D 1997 *Perception* **11** 157–78
- [26] Tolhurst D J and Tadmor Y 1997 *Vision Res.* **37** 3203–15
- [27] Brady N and Field D 1995 *Vision Res.* **35** 739–56
- [28] Brady N 1997 *Perception* **26** 1089–100
- [29] Shannon C and Weaver W 1948 *A Mathematical Theory of Communication* (, IL: University of Illinois Press)
- [30] Mackworth N H and Morandi A J 1967 *Perception Psychophys.* **2** 547–52
- [31] Loftus G R and Mackworth N H 1978 *J. Exp. Psychol.* **4** 565–72
- [32] Rayner K and Duffy S A 1986 *Memory Cogn.* **14** 191–201
- [33] Egeth H and Yantis S 1997 *Annu. Rev. Psych.* **48** 269–97
- [34] Mannan S, Ruddock K and Wooding D 1995 *Perception* **9** 363–86